

Uncertainty propagation of PC-MRI derived inlet boundary conditions in computational hemodynamics models of human aorta

Original

Uncertainty propagation of PC-MRI derived inlet boundary conditions in computational hemodynamics models of human aorta / Bozzi, Silvia; Gallo, Diego; Ponzini, Raffaele; Rizzo, Giovanna; Morbiducci, Umberto; Passoni, Giuseppe. - (2016). (XXXV Convegno Nazionale di Idraulica e Costruzioni Idrauliche IDRA16 Bologna (Italia) 14 - 16 Settembre 2016) [10.6092/unibo/amsacta/5400].

Availability:

This version is available at: 11583/2677965 since: 2017-08-03T09:54:09Z

Publisher:

ICAM - Università di Bologna

Published

DOI:10.6092/unibo/amsacta/5400

Terms of use:

This article is made available under terms and conditions as specified in the corresponding bibliographic description in the repository

Publisher copyright

(Article begins on next page)

UNCERTAINTY PROPAGATION OF PC-MRI DERIVED INLET BOUNDARY CONDITIONS IN COMPUTATIONAL HEMODYNAMICS MODELS OF HUMANAORTA

*Silvia Bozzi*¹, *Diego Gallo*², *Raffaele Ponzini*³, *Giovanna Rizzo*⁴, *Umberto Morbiducci*² & *Giuseppe Passoni*¹

(1) Department of Electronics, Information Science and Bioengineering, Politecnico di Milano, Milan; (2) Department of Mechanical and Aerospace Engineering, Politecnico di Torino, Turin; (3) HPC and Innovation Unit, CINECA, Milan; (4) IBFM, Research National Council, Milan

KEY POINTS:

- The study investigates the impact that uncertainty in PC-MRI derived inlet boundary conditions has on patient-specific computational hemodynamics models of the human thoracic aorta.
- The results show an increase of the uncertainty in fluid dynamics quantities, with respect to the input uncertainty, more marked for blood pressure than velocity and vorticity magnitude.
- The results also show that, overall, there are no preferential locations at the aortic arch where the local hemodynamics is more markedly affected by the uncertainty in measured inflow boundary conditions.

1 INTRODUCTION

Cardiovascular disease (CVD), including heart attack, stroke and peripheral vascular disease, is one of the main cause of death in the world. In the last decades, computational fluid dynamics (CFD) has proved to be an effective tool to gain insights into the relationships between hemodynamics and pathophysiology. More recently, the coupling of computational hemodynamics and cardiovascular imaging has allowed to build up even more realistic and personalized CFD (Taylor & Steinman, 2010). In particular, phase-contrast magnetic resonance imaging (PC-MRI) has been increasingly used to provide patient-specific vessel geometries and flow rate waveforms, useful for setting personalized conditions at boundaries.

However, the reliability of image-based CFD results strongly depends on the level of uncertainty of the simulation parameters and conceptual modelling assumptions. Main sources of epistemic uncertainty of computational hemodynamics are known to be the reconstructed vessel geometry (Sankaran *et al.*, 2016), input and output boundary conditions (BCs) (Morbiducci *et al.*, 2013), vessel elastic properties and motion (Zhao *et al.*, 2010) and blood viscosity rheology models (Lee & Steinman, 2006). All of these modelling assumptions and physical or empirical parameters may lead to marked differences in predicted hemodynamics, possibly limiting translation to clinics.

In this study, we investigate the effect of one of the leading cause of uncertainty in image-based cardiovascular simulations, the PC-MRI derived Dirichlet conditions at inflow boundaries. By means of a set of Monte Carlo simulations, we attempt to provide advice on where, when and how is important to account for inlet BC uncertainty in CFD models of human thoracic aorta. The final goal of the research is to obtain accurate and reliable information useful to diagnostic/prognostic purposes.

2 METHODS

2.1 PCI-MRI data

4D PC-MRI hemodynamic measurements were used to obtain the anatomic model of a healthy human thoracic aorta (Fig. 1a). Details on the *in vivo* PCI-MRI acquisitions and on model reconstruction can be found in Morbiducci *et al.* (2011). The geometry is characterized by an inlet section at the ascending aorta (AAo) and multiple outlets at the descending aorta (DAo) and at the supra-aortic vessels: brachiocephalic artery (BCA), left common carotid artery (LCCA) and left subclavian artery (LSA). Seven cross-sections (perpendicular to the local vessel's axis) were selected along the thoracic aorta, at relevant anatomical landmarks (Fig 1a) and used to evaluate how uncertainty propagates.

Measured phase velocity data were used to obtain three dimensional velocity maps of blood flow at the AAo inflow section and flow rate repartition at the output sections of the model, at multiple phases of the cardiac cycle (Morbiducci *et al.* 2013, Gallo *et al.* 2012). The velocity vector fields retrieved from the PC-

MRI images were used to prescribe inflow boundary conditions at the inlet section of the ascending aorta, as explained in the following section. Fig 1b shows the time history of the average trough-plane and in-plane velocity components at the AAO inlet section.

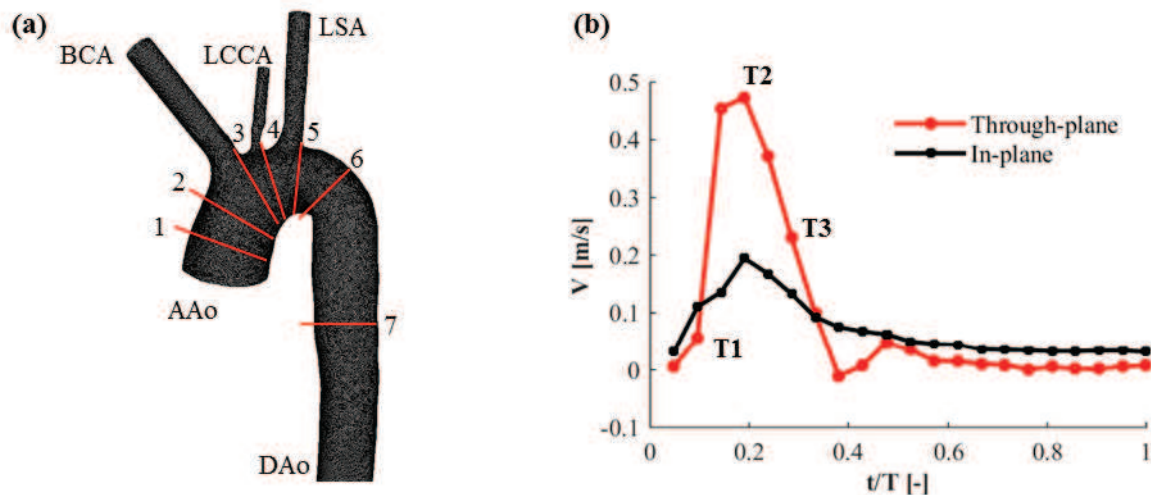


Figure 1. PC-MRI derived model of the thoracic aorta (a). Red lines indicate the positions of the planes used for post-processing. Measured through-plane and in-plane velocities, averaged over the AAO inlet section, during a cardiac cycle of period T . Time instants T1, T2 and T3 are selected for steady-state simulations.

2.2 Fluid dynamic model

The fluid domain was discretized into prismatic and tetrahedral cells. Two unstructured meshes were created with about 5 and 15 million volume elements. Then, blood flow through the aortic arch was simulated using the finite volume CFD code ANSYS Fluent (ANSYS Inc., USA). Three different phases of the cardiac cycle (Fig. 1b) were considered: at the beginning of the systole (T1), at the systolic peak (T2) and halfway of the systolic deceleration phase (T3). The three phases are characterized by a mean Reynolds number at the AAO inlet section, equal to 608, 5138, 2497, respectively. For each time instant, 3D stationary continuity and Navier-Stokes equations were solved without turbulence closure, using second-order accuracy and double numerical precision. The simulations were performed on the 5 million mesh for the instants T1 and T3 and on the finer mesh for phase T2. In both cases, a mesh convergence study was performed to ensure a grid independent solution. Blood was modelled as an incompressible, Newtonian fluid with a density of 1060 kg/m^3 and a dynamic viscosity of 0.0035 Pa s . Arterial walls were assumed to be rigid, with no-slip condition on them. Straight flow extensions were added to the four outlet sections (DAo, BCA, LCCA and LSA) to reduce the effect of the outflow BCs on the solution. A stress-free Neumann condition was imposed at the end of these extensions.

Inlet boundary conditions were derived from phase contrast velocity data by linear interpolation of the discrete PCI-MRI velocity vector maps into the cell centroids of the AAO inlet section (Fig. 2). For each simulated cardiac phase, two different boundary conditions were generated: a 1D velocity profile and a fully 3D profile, which retains all the three component of the measured velocity field.

2.3 Stochastic model

The Monte Carlo method was used to propagate the uncertainty source through the CFD model of the aorta. The three velocity components extracted from the PC-MRI images were assumed to be normally distributed, around the measured values. The random noise - added to PC-MRI measures - was assumed to be normally distributed with zero mean and standard deviation σ corresponding to a signal to noise ratio (SNR) equal to 16 (Tresoldi *et al.* 2014). To achieve statistically reliable results, the number of Monte Carlo runs was determined by increasing the amount of experiments until convergence of the probability density functions (*pdfs*) was reached. The resulting number of realizations was 100.

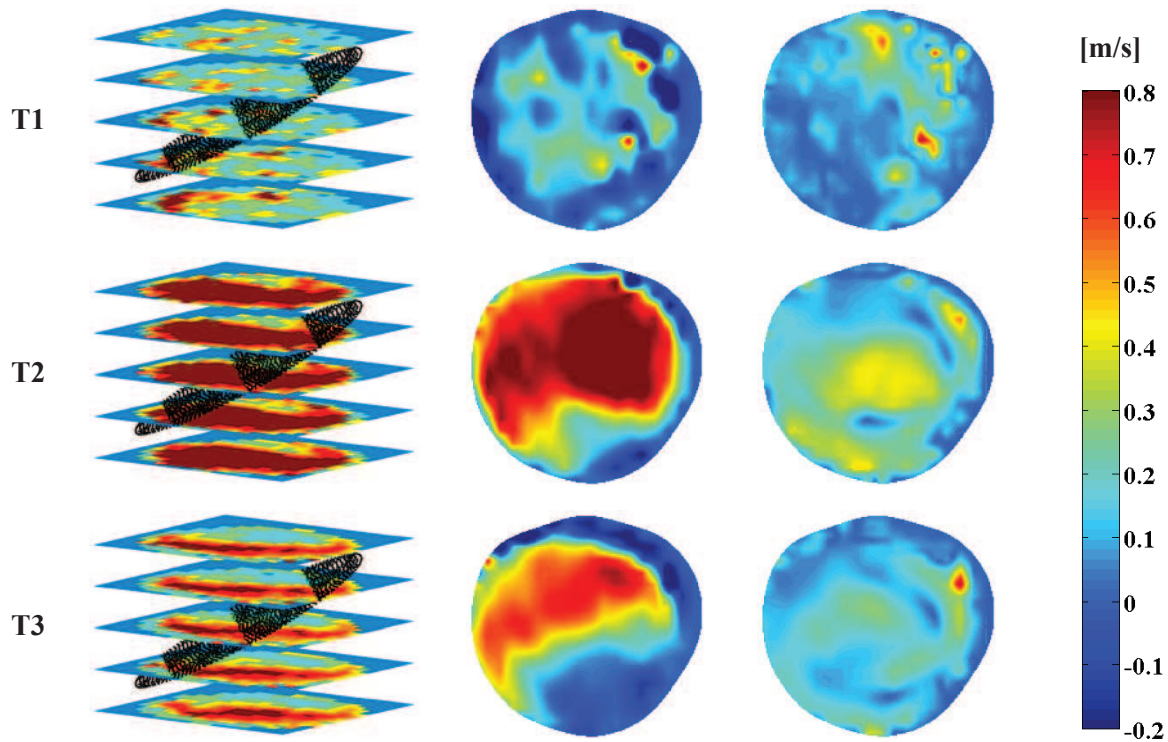


Figure 2. PC-MRI-derived flow data at three cardiac phases. From left to right: PC-MRI velocity measurements and AAO inlet section (black dots correspond to cell centroids), contours maps of through-plane velocity and in-plane velocity at the inflow section.

3 RESULTS

The results of the Monte Carlo simulations were used to estimate the empirical probability density functions of different hemodynamic variables at relevant anatomical singularities. Figure 3 shows the SNR of the *pdfs* at the selected locations along the aorta, from plane 1 (located just downstream of the AAO section) to plane 7 (in the descending aorta) for three flow variables: velocity magnitude (a), pressure (b), and vorticity magnitude (c). The results were obtained prescribing a fully 3D velocity profile at the inlet section of the AAO, but the same conclusions can also be drawn for the 1D inlet BC profile.

It can be noticed that the predicted uncertainty of the three output variables is almost the same for the seven cross-sections. This means that there are no specific locations along the aorta, which are more affected by the inlet BC uncertainty than others. Differently, the results indicate that the magnitude of the output uncertainty depends on the flow variable of interest and to a lesser extent on the cardiac phase. Uncertainty in blood pressure is the highest followed by the uncertainty in velocity and vorticity magnitude. This is generally true for all the phases of the cardiac cycle. The SNR, averaged over the seven analysis planes, for the three phases T1, T2 and T3 was equal to 14, 15 and 14 for velocity magnitude; 9, 9 and 11 for pressure and 15, 13 and 16 for vorticity magnitude. These results show that the magnitude of the predicted uncertainty is always higher than that one of the prescribed input uncertainty (SNR = 16), with the exception of one single case (vorticity magnitude for phase T3). Interestingly, it can be observed that the SNR of blood pressure can be up to 40% lower than the one of the uncertainty source. Regarding uncertainty variability with respect to the cardiac phase, no common trends can be identified for the three flow variables. The SNR of blood velocity magnitude is almost constant for the three cardiac phases, while the SNR of vorticity magnitude exhibits the highest intra-phase variability, with phase T2 being the most affected by uncertainty. Finally, blood pressure uncertainty is higher for phases T1 and T2 than for phase T3.

4 CONCLUSIONS

The main findings of the work are that: (1) propagating the inflow BC uncertainty through the Navier-Stokes equations leads to a decrease in the signal to noise ratio; (2) blood pressure is the hemodynamic

variable, which is more affected by the uncertainty in the inlet BC, followed by velocity and vorticity magnitude; (3) there are no specific aortic locations which are more affected by the inlet BC uncertainty than others; (4) no common trend for the three hemodynamic variables can be identified with regards to the uncertainty magnitude with respect to cardiac phases; (5) the effect of the inflow BC strategy (i.e. 1D or 3D velocity profile) on the *pdfs* of the target variables is negligible. Major limitations of the study rely in the steady flow assumption and in the Neumann condition imposed at the outlet boundaries.

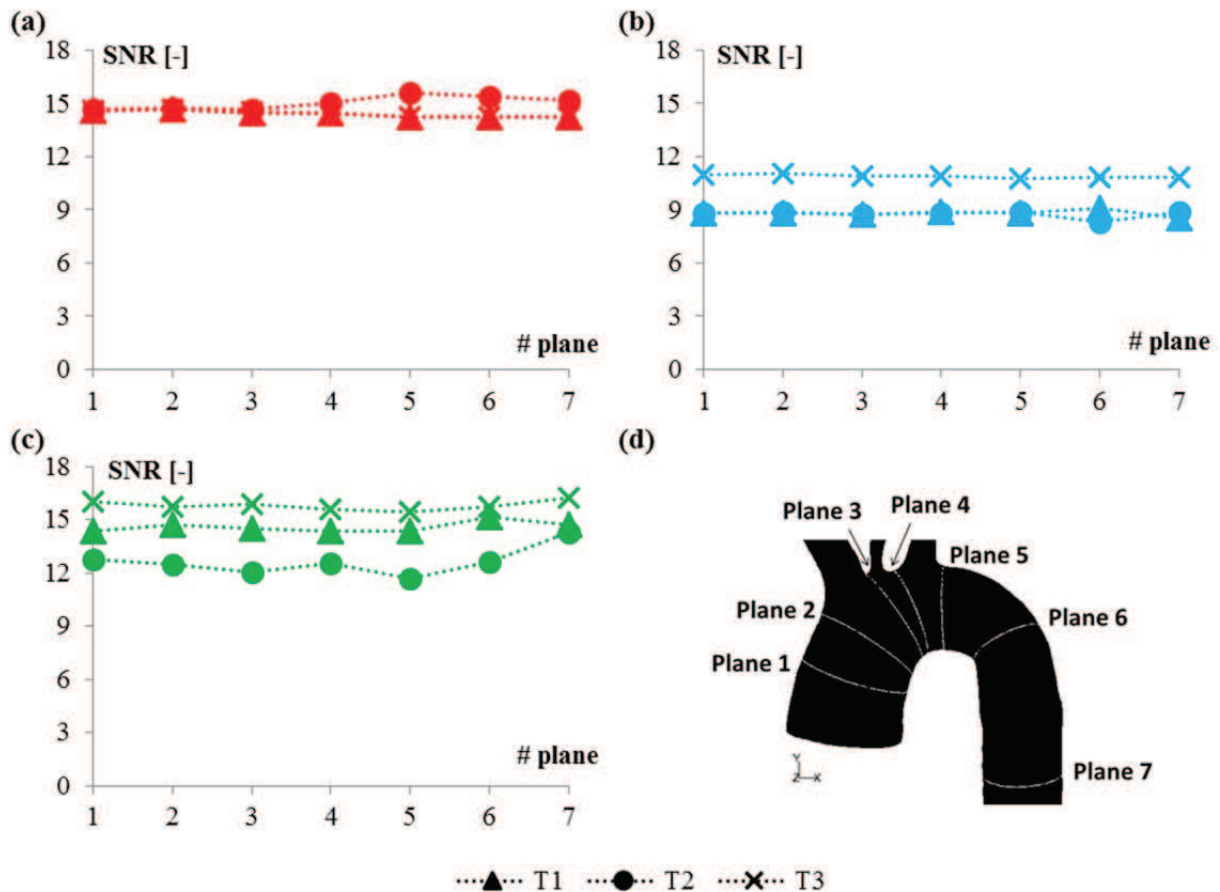


Figure 3. Signal to noise ratio (SNR) of cross-section averaged blood velocity magnitude (a), pressure (b) and vorticity magnitude (c) at different positions along the aorta (d), for three phases of the cardiac cycle.

REFERENCES

Gallo, D., De Santis, G., Negri, F., Tresoldi, D., Ponzini, R., Massai, D., Deriu, M.A., Segers, P., Verhegghe, B., Rizzo, G., & Morbiducci, U. On the use of in vivo measured flow rates as boundary conditions for image-based hemodynamic models of the human aorta: implications for indicators of abnormal flow, *Ann. Biomed. Eng.*, 2012, 40(3), 729–741.

Lee, S.W. & Steinman, D.A. On the Relative Importance of Rheology for Image-Based CFD Models of the Carotid Bifurcation, *J. Biomech. Eng.*, 2007, 129(2), 273–278.

Morbiducci, U., Ponzini, R., Rizzo, G., Cadioli, M., Esposito, A., Montevecchi, F.M. & Redaelli, A. Mechanistic insight into the physiological relevance of helical blood flow in the human aorta. An in vivo study, *Biomech. Model. Mechanobiol.*, 2011, 10, 339–355.

Morbiducci, U., Ponzini, R., Gallo, D., Bignardi, C. & Rizzo, G. Inflow boundary conditions for image-based computational hemodynamics: impact of idealized versus measured velocity profiles in the human aorta, *J. Biomech.*, 2013, 46(1), 102–109.

Sankaran, S., Kim, H.J. Choi, G. & Taylor, C.A. Uncertainty quantification in coronary blood flow simulations: impact of geometry, boundary conditions and blood viscosity, *J. Biomech.*, 2016.

Taylor, C.A. & Steinman, D.A. Image-based modelling of blood flow and vessel wall dynamics: applications, methods and future directions, *Ann. Biomed. Eng.*, 2010, 38(3), 1188–1203.

Tresoldi, D., Cadioli, M., Ponzini, R., Esposito, A., De Cobelli, F., Morbiducci, U. & Rizzo G. Mapping aortic hemodynamics using 3D Cine Phase Contrast Magnetic Resonance parallel imaging: evaluation of an anisotropic diffusion filter. *Magn. Res. Med.*, 2014, 71, 1621-1631.

Zhao, S.Z., Xu, X.Y., Hughes, A.D., Thom, S.A., Stanton, A.V., Ariff, B. & Lon, Q. Blood flow and vessel mechanics in a physiologically realistic model of a human carotid arterial bifurcation, *J. Biomech.*, 2000, 33(8), 975–984.